Published online November 27, 2005

Nucleic Acids Research, 2005, Vol. 33, No. 20 ***e177***
doi:10.1093/nar/gni174

Bis-aptazyme sensors for hepatitis C virus replicase and helicase without blank signal

Suhyung Cho[1], Ji-Eun Kim[2], Bo-Rahm Lee[2], June-Hyung Kim[2] and Byung-Gee Kim[1,2,*]

[1]Interdisciplinary Program for Biochemical Engineering and Biotechnology and [2]School of Chemical and Biological Engineering, Seoul National University, Shinlim-dong, Kwanak-Gu, Seoul 151-744, Korea

Received May 31, 2005; Revised August 27, 2005; Accepted October 18, 2005

ABSTRACT

The fusion molecule (i.e. aptazyme) of aptamer and hammerhead ribozyme was developed as *in situ* sensor. Previously, the hammerhead ribozyme conjugated with aptamer through its stem II module showed a significant blank signal by self-cleavage. To reduce or remove its self-cleavage activity in the absence of target molecule, rational designs were attempted by reducing the binding affinity of the aptazyme to its RNA substrate, while maintaining the ribonuclease activity of the aptazyme. Interestingly, the bis-aptazymes which comprise the two aptamer-binding sites at both stem I and stem III of the hammerhead ribozyme showed very low blank signals, and their ratios of reaction rate constants, i.e. signal to noise ratios, were several tens to hundred times higher than those of the stem II-conjugated bis-aptazymes. The reduction in the blank signals seems to be caused by a higher dissociation constant between the main strand of the bis-aptazyme and its substrate arising from multi-point base-pairing of the bis-aptazymes. The bis-aptazymes for HCV replicase and helicase showed high selectivity against other proteins, and a linear relationship existed between their ribozyme activities and the target concentrations. In addition, a bis-aptazyme of dual functions was designed by inserting both aptamers for HCV replicase and helicase into the stem I and stem III of hammerhead ribozyme, respectively, and it also showed greater sensitivity and specificity for both proteins without blank signal.

INTRODUCTION

Analysis of cancer markers or disease related proteins has become important issue in prognosis, diagnosis and treatment of cancer and disease (1,2). For the detection of such specific proteins in blood and tissue, antibody (Ab) is the most common reagent used in autoradiography, enzyme-linked immunosorbent assay (ELISA) and western blotting. Advantages and drawbacks in using Ab are well documented. For example, the use of secondary Ab in sandwich assay requires Ab conjugated with enzyme or fluorescent dye. Ab reaction usually takes time and requires specific reaction conditions for binding of target molecules. In addition, some antibodies are temperature-sensitive, so that they are easily degraded during long time handling. Therefore, development of alternative, fast, temperature-resistant, sensitive and high-throughput non-isotopic analytical methods to selectively detect target molecules from complex mixtures is very much in need and challenging (3). Recently, aptamers were introduced as a substitute for Abs in the application of biosensors for detection and measurement of biological or environmental molecules (4–9), because aptamers can be easily developed for molecules for which we cannot generate Abs. As aptamers are rapidly matured through *in vitro* evolution method (10), they show almost equivalent or even better dissociation constants, compared with Abs. As a variation of aptamer, aptazyme (or called allosteric ribozyme) was developed as an *in situ* biosensor (7). Since the aptazyme is a conjugated molecule between aptamer and ribozyme, we can extract only the beneficial properties of both aptamer and ribozyme, i.e. high-binding affinity and sequence-specific nucleotide cleaving activity (11). Various aptazymes were designed to transduce the binding energy of small analyte molecules (12–14) or macromolecules (15) or proteins (16) into the activation energy of the catalytic activity of ribozyme (7,17–19). When aptazymes are used as biosensors, sensitive detection is possible by signal amplification even at low target concentrations, because the catalytic activity of the aptazymes can be easily amplified by serial addition of the corresponding substrate.

On the contrary, the disadvantages of using aptazymes as biosensors are such that (i) maintaining complete binding affinity of aptamer moiety as well as the intact activity of ribozyme moiety is not easy, (ii) aptazymes sometimes show relatively high blank signals owing to the inherent self-cleaving activity of ribozyme (20,21). The issue of

*To whom correspondence should be addressed at Laboratory of Molecular Biotechnology and Biomaterials, School of Chemical and Biological Engineering, Seoul National University, Shinlim-dong, Kwanak-Gu, Seoul 151-744, Korea. Tel: +82 2 880 6774; Fax: +82 2 883 6020; Email: byungkim@snu.ac.kr

high blank activity is very critical to develop the aptazyme as biosensor, because the blank signal suppresses the sensitivity of sensor and the limit of detection range. To solve this problem, optimum aptazymes were screened and selected by randomizing the sequence of linking module or total aptazyme to reduce or remove the self-cleavage effect (21). However, the *in vitro* evolution method is time-consuming to develop and difficult to apply for other molecules except the selected target. As high-throughput screening of aptamers driven by automation of *in vitro* selection method (22) and a database of reported aptamers (23) are provided, developing easy and rather simple, but general design principles to make aptazymes without blank signal, would be very useful to change them into smart biosensors.

Here, we introduce a new design principle of aptazymes to eliminate blank signal, and to enhance the catalytic activity based upon the mechanism of self-cleaving hammerhead ribozyme. Most previous approaches in constructing allosteric fusion aptazyme were done through conjugation of the stem II of hammerhead ribozyme, since the stem II region was known to be the most sensitive module in exerting the ribozyme activity (24). Unfortunately, the high sensitivity of the stem II module in aptazymes often greatly influences to yield high blank signal of the self-cleavage activity. Therefore, rather less sensitive moiety of stem I or stem III region was used for the conjugation with aptamers. Surprisingly, inserting aptamers in both stem I and stem III regions made the aptazymes very stable and sensitive. In this paper, using aptamers for HCV replicase and HCV helicase and hammerhead ribozyme as model systems, we would like to explain how the fusion aptazymes are constructed, and why the fused aptazymes are more stable without blank signal and even more sensitive to target molecules. This kind of approach in designing aptazymes will be very useful for the development of *in situ* biosensors, protein chips and gene therapy.

MATERIALS AND METHODS

Preparation of aptazyme

All single-stranded DNA (ssDNA) strands were synthesized and purified by PAGE from IDT (Coralville, IA) and Cosmo Co. (Seoul, Korea). ssDNA strands containing T7 promoter region in 5′ end region were amplified by PCR with 5′ primer and 3′ primer. After gel purification of DNA product, template RNAs (Table 1) were prepared by *in vitro* transcription using T7 RNA polymerase. All the RNA transcripts were separated by 6% PAGE gel containing 8 M urea after phenol extraction and ethanol precipitation. The purified RNAs once again were dissolved in 0.1% diethylpyrocarbonate and stored at −80°C for further experiments. The substrates for the aptazymes were dual-labeled with 6-carboxyfluorescein (6-Fam) and 4-dimethylaminoazobenzene-4′-sulfonyl chloride (dabcyl) at 5′ and 3′ ends, respectively, and the 6-Fam-5′-AGCCGUCUCG-GUU-3′-dabcyl of 13mer and 6-Fam-5′-CCGGGGUCUCGG-GGCC-3′-dabcyl of 16mer synthetic RNAs were purchased from IBA (Goettingen, Germany).

Purification of HCV replicase and helicase protein

pET21a vectors cloned with HCV replicase and HCV helicase were transformed into BL21(DE3) and the host cells were cultured at 37°C. To over-express the proteins, 0.2 mM isopropyl-β-D-thiogalactopyranoside was added to the cell culture media at ∼0.5 of cell density (OD_{600}). After 5 h from the induction, the cells were harvested and the cell extract was prepared by sonication in the 50 mM phosphate buffer containing 1 mM phenylmethylsulfonyl fluoride and 1 mM EDTA for 20 min. The proteins containing six consecutive histidine residues at their C-terminals were purified with Ni-NTA agarose resin (Qiagen, Hilden, Germany). Imidazole buffer (250 mM) used for the protein elution was removed by dialysis against phosphate-buffered saline buffer, and quantitative analysis of the proteins was performed by Bradford assay.

The activity assay of aptazyme

Before the reaction with target protein, to retain RNA structure in the binding buffer [10 mM Tris–HCl, 100 mM KCl and 10 mM $MgCl_2$ (pH 7.6)], all the aptazymes used were pre-incubated for 10 min at room temperature after heating at 80°C for 3 min. Each 1 μM designed aptazyme was reacted with target protein for 20 min at room temperature. The aptazyme and protein mixture were transferred to a 50 μl cuvette, the reaction was started by adding 1 μM substrate. Reaction kinetics of the aptazyme was measured by fluorospectrometer (Jasco, Tokyo, Japan). All the measurements were performed in the binding buffer at 496 nm excitation wavelength and 516 nm emission wavelength (slit excitation size, 10 nm; slit emission size, 10 nm). The reaction rate constant was obtained by calculating $\{\ln[(F_t - F_i)/F_i]/\Delta t\}$ at each protein concentration, assuming a first-order kinetics. Here, F_t and F_i are the

Table 1. The sequences of designed aptazymes

Conjugation	RNA sequences
Stem II (R)	GGCCGACUGAUGAUGAGCUGGGCCACAUUGUGAGGGGCUCAGCGAAACGGCU
Stem II (H)	GGCCGACUGAUGAUGAGCUGCCAGUAGUGUAUAGGGCAGCGAAACGGCU
Stem I (R)	GGCCACGCGCCACAUUGUGAGGGGCGCGACCGACUGAUGAU GAGCGAAAGCGAAAACCCCGG
Stem III (H)	GGCCCCGACUGAUGAUGAGCGAAAGCGAAACCCAGCCAGUAGUGUAUAGGGCACGG
Stem I/III (R–R)	GGCCACGCGCCACAUUGUGAGGGGCGCGACCGACUGAUGAUGAGCGAAAGCGAAACCCAGGCGCCACAUUGUGAGGGGCGCCACGG
Stem I/III (H–H)	GGCCAGGGCAGUAGUGUAUAGGCCCACCGACUGAUGAUGAGCGAAAGCGAAACCCAGCCAGUAGUGUAUAGGGCACGG
Stem I/III (R–H)	GGCCCCGACUGAUGAUGAGCUGGGCCACAUUGUGAGGGGCUCAGCGAAACCCAGGCCAGUAGUGUAUAGGGCCACGG

R, aptazyme for HCV replicase, H, aptazyme for HCV helicase.

fluorescence intensities at 5 and 0 min, respectively. The ratio of rate constants was defined as the ratio of the reaction rate constant in the presence of target protein to that in the absence of target protein.

Analysis of interaction of bis-aptazyme and substrate

To measure the relative cleavage activities of the modified hammerhead ribozymes, primary amine modified mutant substrate (NH_2-C_6-CCGGGGUGUCGGGGCC) (IDT, Coralville, IA) for the hammerhead ribozyme was immobilized on CNBr agarose beads with the binding capacity of 7 mmol/10 µl (Sigma, St Louis, MO) in 50 mM sodium bicarbonate buffer (pH 8.0) for 2 h at room temperature. The residual functional group on the bead was subsequently blocked by 1 M ethanolamine for overnight at 4°C. The substrate-bound beads were washed three times by 50 mM sodium bicarbonate buffer and two times by the reaction buffer [10 mM Tris–HCl, 100 mM KCl and 10 mM $MgCl_2$ (pH 7.6)]. Bis-aptazymes were labeled with dUTP-fluorescein using a terminal deoxynucleotidyl transferase (Roche, Mannheim, Germany). The modified bis-aptazyme was separated by 8 M urea 6% PAGE, and its total amount was measured by fluorospectrometer after elution. Before binding to the beads, the fluorescence labeled bis-aptazyme was incubated for 3 min at 80°C and stored for 10 min at room temperature for stable RNA structure conformation. Aptazymes (20 pmol) were added to the beads and reacted for 5 min at room temperature under mild mixing. The beads were subsequently washed five times with binding buffer, and then the 3 µl beads were transferred to a slide glass, and observed at the same laser intensity with laser-scanning confocal fluorescence microscopy (Bio-Rad MRC 1024, Bio-Rad Laboratories Inc., CA). The fluorescence microscopy used a krypton/argon laser for excitation at 488 nm.

RESULTS

The design of aptazymes for HCV replicase and HCV helicase

General strategy for developing aptazymes using hammerhead ribozyme was to fuse the binding site of target aptamer into the stem II region of the ribozyme (Figure 1a). It was based upon the prediction of stable structure maintaining their original structures of aptamer and ribozyme with the lowest conformational energy (ΔG_{conf}) (7,17). The other strategy was to select optimized aptazymes showing high ribonuclease activities upon binding target molecule through serial *in vitro* selection by randomizing the residual sequences except the conserved minimal sequences of ribozyme (8,17). In our study, the former strategy of rational design was adopted because of its general applicability to any target molecules.

Primarily, we attempted to fuse the protein-binding region of HCV replicase aptamer into the stem II region of the hammerhead ribozyme. The structure of HCV replicase aptamer has two loop–stem structures, and the sequences of the target protein-binding sites in the two loops are GGCCACAUUGUGAGGGGCUC and GGAUCGCAUGGCCGUGUCC (Supplementary Figure 1Sa). If we include the complete

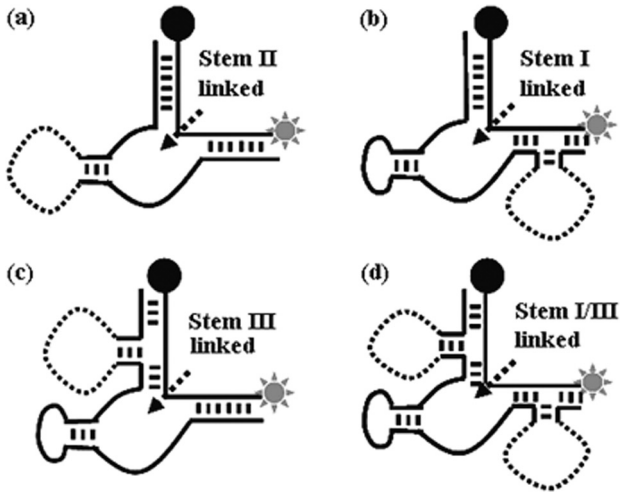

Figure 1. Schemes of various aptazymes designed through conjugation with the three stems of hammerhead ribozyme (**a**) stem II linked aptazymes, (**b**) stem I linked aptazymes, (**c**) stem III linked aptazymes and (**d**) stem I/III linked aptazymes.

sequences of the aptamer and the ribozyme, the total length of the fusion conjugate would become 85mer. Since long sequence of aptazyme often significantly decreases the activity of ribozyme (25), and requires a high cost in the synthesis of the aptazyme, shorter and stabler aptazyme is preferred in applying it to biosensors. Three kinds of aptazymes were designed by changing the protein-binding sequences of the aptamer moiety for the connection of the stem II region of the hammerhead ribozyme: the 85mer with two binding sites (type II-A) (Supplementary Figure 1Sa), the 52mer with the left-hand binding site (type II-B) (Supplementary Figure 1Sb) and the 52mer with the right-hand binding site (type II-C) (Supplementary Figure 1Sc). The secondary structure of each aptazyme was predicted by 'RNA structure version 4.1' (26). The dissociation constant (K_d) of each aptazyme for the HCV replicase was measured using surface plasmon resonance. The dissociation constants of type II-A, type II-B and type II-C aptazymes for the HCV replicase were 0.43, 4.43 and 2.90 nM, respectively, suggesting that the aptazyme comprising the complete binding sites of the replicase yields 10 times higher binding affinity than the one only with the left-hand side of the binding sites. To find out any relationship between the binding affinity of the aptazyme and its ribozyme activity, the catalytic activity of each aptazyme was measured by fluorescence spectrometry in the presence of 100 nM HCV replicase (Supplementary Figure 2S). Type II-B aptazyme showed 2 and 3.5 times higher ribozyme activities than type II-A and type II-C, respectively. Although the type II-A showed 10 times higher binding affinity to the replicase, there is no direct correlation between the binding affinity and the ribozyme activity. Rather, the ribozyme activity of the aptazyme appears to have a close relationship with conformational or structural changes around its catalytic site such as the compactness of ribozyme (25,27), length of stem (19) and stable secondary structure. Despite the higher binding affinity of type II-A, the longer sequence of type II-A seems to reduce its ribozyme activity. Although the affinity of type II-B is 10 times lower than that of type II-A, low nanomolar range dissociation constant is still effective enough to be used as a

biosensor to detect any target molecules. In result, type II-B aptazyme showing the highest ribozyme activity was selected for further study on the design of the aptazyme for HCV replicase.

The aptamer for HCV helicase had the binding site of beacon shape with one loop and one stem (28). For the conjugation of the HCV helicase aptamer with the hammerhead ribozyme, the helicase-binding site 'GCAGUAGUGUAUAGGC' in the loop was inserted into the stem II of the hammerhead ribozyme, maintaining the original structure of the aptamer and the ribozyme (Table 1).

Characteristics of conjugated aptazymes for HCV replicase and HCV helicase

In the case of the conjugated aptazymes through the stem II region of the hammerhead ribozyme, one interesting observation was that the blank signals in the absence of any target proteins were very high owing to the high self-cleavage activity of the aptazymes (Supplementary Figure 2S). Hammerhead ribozyme naturally has the self-cleavage activity in metal containing solution (24), and the stem II module of the hammerhead ribozyme is known to be the most sensitive module in determining its catalytic activity. To avoid such high blank signals for the stem II conjugated aptazymes, the stem I or/and stem III of the hammerhead ribozyme was/were attempted for the conjugation. We expected that less tight complementary binding of the ribozyme substrate may induce some reduction in the self-cleavage activity of the conjugated aptazyme. With the selected binding regions of the aptamers for HCV replicase and HCV helicase, conjugated aptazymes were constructed by fusing the sequence of the binding regions into the stem I, II, III and I/III of the hammerhead ribozyme (Figure 1). Their RNA sequences are shown in Table 1. The substrate sequence of the stem II conjugated aptazymes was 13mer RNA, and those of stem I, stem III and stem I/III were 16mer RNAs labeled by 6-Fam at 5′ end and dabsyl at 3′ end. All the aptazymes were selected to preserve the original structures of the aptamer-binding site and ribozyme active site and to have the lowest Gibbs free energy in secondary structure prediction (Supplementary Figure 3S). The activities of the stem II, stem I or/and III-conjugated aptazymes for target proteins were measured using the same sequence substrate. When the target molecule binds to the aptamer moiety, the fluorescence intensity from 6-Fam increases over time as the ribozyme moiety becomes functional. All the aptazymes showed a somewhat linear relationship between the ribozyme activity and the concentration of target proteins (Figure 2). To compare the sensitivity of the detection, i.e. signal to noise ratio, the ratio of relative reaction rate constants was used (The activity assay of aptazyme).

In most cases of the mono-aptazymes conjugated with either stem I, stem II or stem III of the hammerhead ribozyme, the blank activities for HCV replicase and helicase were nearly >70% of the activities of the corresponding mono-aptazyme within the ranges of the detection (50–500 nM) of HCV replicase and helicase, respectively. Although the absolute values of the reaction rate constants of the bis-aptazymes did not change greatly (i.e. ~25–40% increase), their ratios of the rate constants changed dramatically because the blank rate constants in the absence of target proteins were greatly

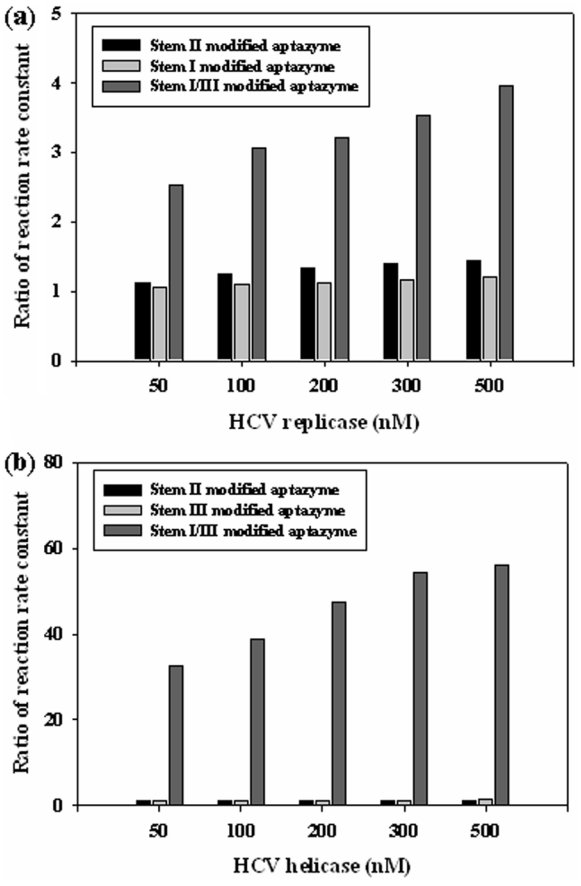

Figure 2. The ratio of reaction rate constants of (**a**) stem II, stem I and stem I/III modified aptazymes for HCV replicase and (**b**) stem II, stem III and stem I/III modified aptazymes at 10 mM Tris–HCl, 100 mM KCl and 10 mM $MgCl_2$ (pH 7.6). The ratio of reaction rate constants means 'the ratio of the rate constant in the presence of protein to that in the absence of protein'. The concentrations of the aptazymes and substrate in the reaction mixture are 1 μM. Reaction rate constants were obtained from $\{\ln[(F_t - F_i)/F_i]/\Delta t\}$ (F_t and F_i are the fluorescence intensities at 5 and at 0 min, respectively). The blank rate constant of stem II mono-aptazyme, stem I mono-aptazyme and stem I/III bis-aptazymes in the absence of HCV replicase were 0.660, 0.757 and 0.254 min^{-1}, respectively. And the blank rate constants of the stem II mono-aptazyme, stem III mono-aptazyme and stem I/III bis-aptazymes in the absence of HCV helicase (b) were 0.715, 0.782 and 0.019 min^{-1}, respectively.

reduced (Figure 2). The blank rate constants of stem II, stem I mono-aptazymes and stem I/III bis-aptazyme in the absence of HCV replicase were 0.660, 0.757 and 0.254 min^{-1}, respectively. The same blank rate constants of the stem II, stem III mono-aptazymes and stem I/III bis-aptazyme in the absence of HCV helicase were 0.715, 0.782 and 0.019 min^{-1}, respectively. The ratios of the rate constants of the bis-aptazyme for HCV replicase and helicase were ~4 and 50 times higher than that of the corresponding mono-aptazymes, respectively. This result suggests that designing bis-aptazymes with high activity to target molecules and very low blank signals at the same time would become a useful approach to improve the function of target aptazymes.

In addition, the substrate specificity of bis-aptazymes for HCV replicase and HCV helicase were examined. The relative activity, i.e. the ratio of rate constants, of the bis-aptazymes were compared in the presence of 200 nM of ovalbumin, BSA, HCV replicase, HCV helicase and these four protein mixtures.

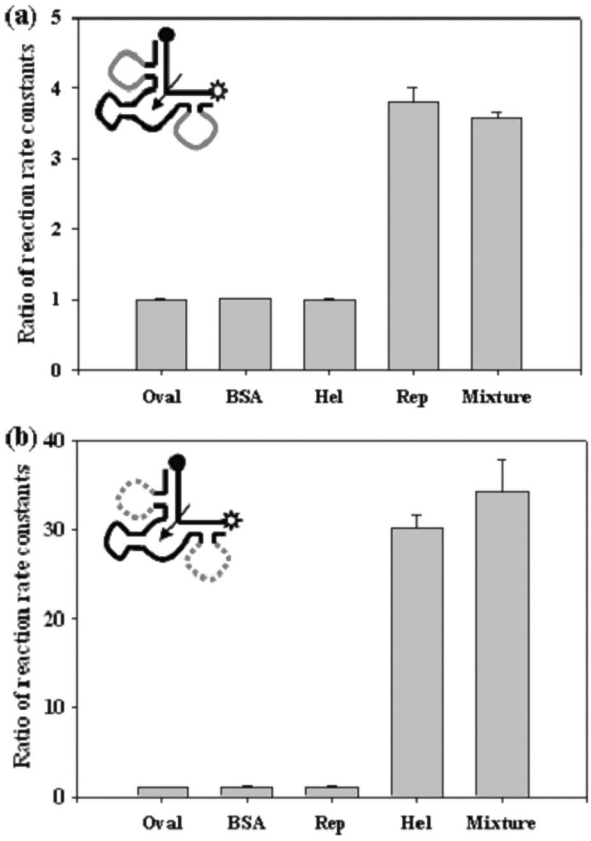

Figure 3. The substrate specificity of the bis-aptazymes for (**a**) HCV replicase and (**b**) HCV helicase. Protein concentrations for the assay were 200 nM of ovalbumin (Oval), BSA, HCV replicase (Rep) and HCV helicase (Hel). The mixture solution consists of 200 nM of all the above protein solutions. Here, the blank rate constants of bis-aptazymes at (a) and (b) were 0.095 and 0.020 min^{-1}, respectively.

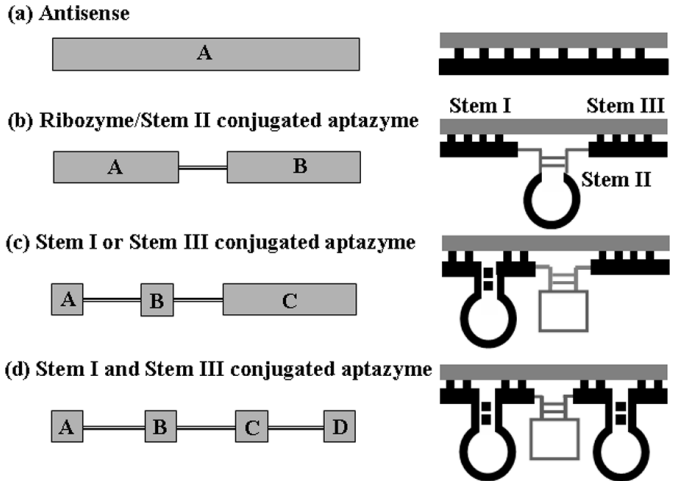

Figure 4. Various types of complementary base-pairing: (**a**) antisense type, which has one long complementary base-pairing A fragment; (**b**) the type of ribozyme or stem II-conjugated mono-aptazyme, having separated two short complementary base-pairing fragments of A and B; (**c**) the type of aptazyme conjugated with either the stem I or stem III of hammerhead ribozyme, having three shorter complementary base-pairing fragments of A, B and C; and (**d**) the type of bis-aptazyme conjugated in the middle of the stem I and stem III of hammerhead ribozyme, having the shortest four complementary base-pairing fragments of A, B, C and D.

As expected, the bis-aptazymes showed its ribozyme activity only in the presence of its corresponding target proteins (Figure 3). The bis-aptazyme activities for HCV replicase and helicase in BSA and ovalbumin known to have high nonspecific binding were nearly similar to the blank activity in the absence of the target protein. The activities of the bis-aptazymes in the protein mixture were almost the same as that for the specific target protein alone. Figure 3 also shows that at 200 nM of each target protein, the aptazyme for HCV helicase is more selective than that for HCV replicase by about five times. Here, the blank rate constants of bis-aptazymes at Figure 3a and b were 0.095 and 0.020 min^{-1}, respectively. The result clearly shows that the bis-aptazyme is very specific and more selective to detect the target molecules.

Why does the bis-aptazyme show low blank signal?

Kinetic mechanism of the hammerhead ribozyme can be dissected into three steps as follows: (i) the complementation between ribozyme main strand and substrate, (ii) self-cleavage of the substrate and (iii) subsequent releasing of the cleaved substrate (29). In fact, the self-cleavage reaction of the hammerhead ribozyme starts upon the completion of complementary binding of the substrate sequence. By introducing an aptamer in the complementary base-pairing region, i.e. the stem I or III domain of the ribozyme, the substrate is expected to show a lower binding affinity to the main strand owing to reduction in the size of the base-pairing sequence. When schematic diagram of sense–antisense base-pairing is given as in Figure 4a, the most common stem II conjugated aptazyme construct would be similar to the schematic diagram in Figure 4b. Here, the complementary pairing fragments are divided into two: A and B. To make a construct of lower binding affinity having shorter complementary sequences in the ribozyme, conjugating an aptamer in either the stem I or stem III region is possible (Figure 4c). Then the complementary pairing fragments are divided into three parts: A, B and C. Similarly two aptamers can be inserted into both stem I and stem III regions (Figure 4d). Now, the bis-aptazyme is divided into four short base-pairing fragments. As the number of fused aptamers increases, the number of fragments of short complementary base-pairings increases, resulting in a decrease in the total number of base pairs involved in the assembly. Binding affinity based upon the Gibbs free energy of the complementary base-pairings would decrease in the order of (b), (c) and (d) in the absence of the target protein (Table 2). However, since the aptamer can rapidly change the secondary structure of the aptazyme itself upon binding with its target protein, the changes in the complementary base-pairing is hard to predict only with the Gibbs free energy calculated based on the number of base-pairings under the static condition before the conformational change.

We wanted to examine whether or not the low blank signal of the aptazyme in Figure 4d is caused by (i) the decrease in the number of the complementary base pairings between the bis-aptazyme and the substrate in the absence of the target protein, or alternatively, (ii) the subsequent conformational changes in the aptazyme–substrate complex that occur upon the binding of the target molecule after the completion of the complementary base pairings between the bis-aptazyme and

Table 2. The affinity constants of sense/antisense RNA pairs

K_a	Antisense	Ribozyme or aptazyme (stem II)	Monoaptazyme (stem I)	Monoaptazyme (stem III)	Biaptazyme (stem I/III)
K_a^I	1.635×10^{29}	5.468×10^{9}	2.252×10^{5}	2.475×10^{12}	2.252×10^{5}
K_a^{II}		2.475×10^{12}	1.4045	1.254×10^{3}	3.81×10^{2}
K_a^{III}			5.468×10^{9}	15.147	1.2543×10^{3}
K_a^{IV}					15.147
${}^aK_{a_{total}}$	1.635×10^{29}	1.353×10^{22}	1.729×10^{15}	4.701×10^{16}	1.630×10^{12}

Equilibrium constants (K_a) were calculated from Gibbs free energies of RNA-RNA interactions. The RNA-RNA interactions were obtained from the RNA secondary structure prediction based on free energy minimization using RNA structure program (4.1 version).
${}^aK_{a_{total}} = K_a^I \times K_a^{II} \times K_a^{III} \times \cdots \times K_a^n$.

the substrate. Experimental designs to prove such changes in the binding affinity of the substrate upon the binding of the target molecule is not easy or simple, because the degree of base-pairing cannot be compared, once the substrate is cleaved by its ribozyme activity. The hammerhead ribozyme usually cleaves the non-complementary sequence in the middle of its stem I and stem III regions except the guanine ribonucleotide (rG). Using this property, a mutant substrate, whose cleavage site is replaced with rG, was designed to compare the changes in the binding affinity to the main strand of the bis-aptazyme in the presence of the target protein (Figure 5a). The mutant substrate (100 pmol) with six-carbon linker at 5′ end was immobilized on CNBr modified agarose beads (7 mmol/10 µl). Subsequently, the 20 pmol bis-aptazyme labeled with fluorescein dye was reacted for 5 min with the immobilized mutant substrate in the presence or absence of the target proteins. Interestingly, the bis-aptazyme did not nearly bind with the mutant substrate without the target proteins (Figure 5b, cases II and V). However, in the presence of the target protein, the bis-aptazyme binds with the mutant substrate very efficiently (Figure 5b, cases III and VI), suggesting that the low blank signal of the bis-aptazymes is originally produced owing to the lower degree of base-pairing between the bis-aptazyme and the substrate. This result also suggests that the main strand of the bis-aptazyme exposes its complementary binding sequence to the mutant substrate only when the target protein binds to the aptamer moiety of the bis-aptazyme, suggesting a true allosteric effect of the aptamer is in function to control the ribozyme activity.

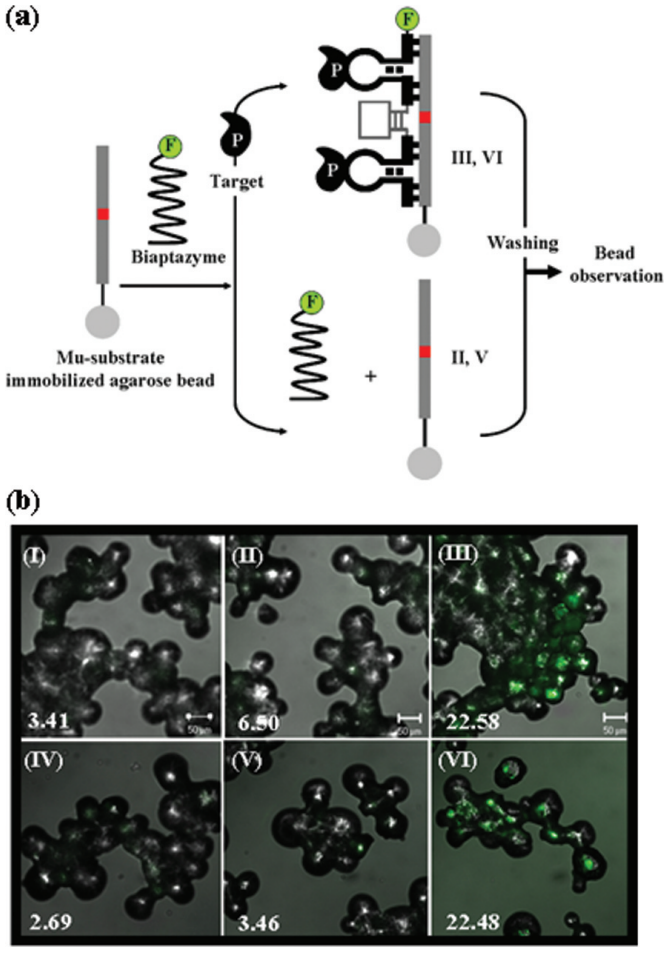

Figure 5. (**a**) The schematic representation of binding test of the bis-aptazyme and substrate sequence in the presence/absence of target protein. The cleavage site of substrate, rC, was changed to uncleavage site, rG (red box). The fluorescence labeled bis-aptazymes were reacted with an immobilized mutated substrate (Mu-substrate) for 5 min. The fluorescence of the beads were observed after washing. (**b**) Laser confocal microscopic analyses of the interaction between 20 pmol fluorescence-labeled bis-aptazyme main strand with 100 pmol substrate were carried out in the presence or in absence of 500 nM target proteins. I and IV are the bead images after the reactions of the bis-aptazymes for HCV replicase and helicase, respectively, on the bare agarose beads without the substrate sequence. II and V are the beads images after the reactions of the same bis-aptazymes for HCV replicase and helicase, respectively. with the substrate in the absence of the target proteins. III and VI are the same bead images as II and V except the reaction in the presence of their target proteins. All the data were obtained after 5 min of hybridization reaction and subsequent five times washing with the solution mixture of 10 mM Tris–HCl, 100 mM KCl and 10 mM $MgCl_2$ (pH 7.6). The numbers on the figure represent the average fluorescence intensity from the beads.

Design of bis-aptazyme for dual detections

As a next step to construct any possible bis-aptazymes, design of hetero-bis-aptazyme which can detect two target molecules simultaneously was attempted. To create the hetero-bis-aptazyme detecting both HCV replicase and helicase with only one aptazyme, the target-binding domain of each aptamer were coupled to the stem I and stem III of the hammerhead ribozyme following the previous design of the stem I/III conjugated bis-aptazyme. Here, each aptamer for HCV replicase and HCV helicase was inserted into the middle of the stem I and stem III, respectively (StemI/III(R–H) (Table 1).

The ratio of rate constants of the hetero-bis-aptazyme was compared at 200 nM of ovalbumin, BSA, HCV replicase, HCV helicase, and the mixture of HCV replicase and helicase (Figure 6). The hetero-bis-aptazyme showed a somewhat comparable activity with the homo-bis-aptazymes conjugated with the two identical aptamers in the stem I and stem III in the presence of HCV replicase or helicase. One interesting

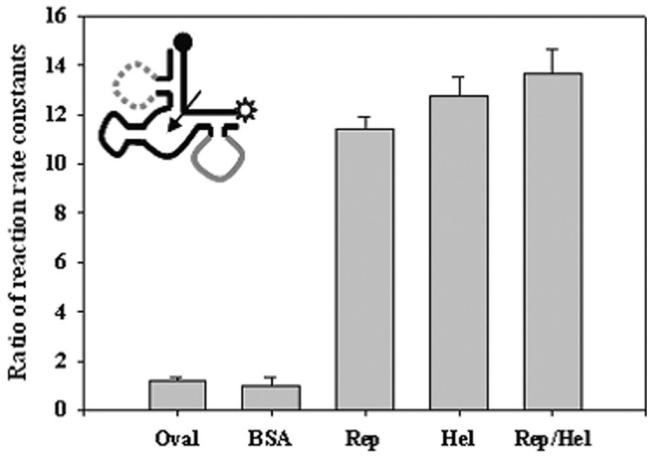

Figure 6. The hetero-bis-aptazyme having two aptamer regions for HCV replicase and helicase into stem I and stem III of one hammerhead ribozyme, respectively, was designed, and its activities were compared for 200 nM ovalbumin (Oval), BSA, HCV replicase (Rep), HCV helicase (Hel), and the mixture of 200 nM HCV replicase and 200 nM HCV helicase (Rep/Hel). The blank rate constant of the hetero-bis-aptazyme in the absence of the two proteins was 0.091 min^{-1}.

observation is that the ratio of the rate constants of hetero-bis-aptazyme of the dual functions does not agree with additive values of the two homo-bis-aptazymes in the presence of the mixture of HCV replicase and HCV helicase, but its value is rather in the middle of the two homo-bis-aptazymes (refer to Figures 3 and 6), suggesting that its selectivity to the target proteins are somewhat averaged out with yet unknown reasons. The nonspecific activities of the bis-aptazyme for ovalbumin and BSA were very low and its blank signal was quite low like that of the above homo-bis-aptazymes. The results indicate that a single molecule, i.e. bis-aptazyme alone, can be easily and efficiently developed as sensors for multiple targets.

Especially, HCV replicase and HCV helicase are NS5b and NS3 proteins of HCV virus, expressed during its infection into the host cells. As the concentrations of the antigen proteins might be very low during the early stage of the infection, it would be difficult and challenging to detect them with normal ELISA assay. If there are any means to amplify the detected signals for the target proteins, improved diagnosis would be possible with minute quantity of patient sample. The hetero-bis-aptazyme of dual functions shown in this study is quite suitable for this purpose, and can be used to detect both target proteins allowing the presence of HCV, and signal amplification is possible with longer analysis time by simply adding more ribozyme substrate.

DISCUSSION

In this study, fusion aptazyme combining aptamer and ribozyme was developed as an *in situ* sensor for the detection of HCV virus related proteins. The aptazyme shows target-specific catalytic ribozyme activity upon binding to the target molecules such as HCV replicase and helicase. To apply the aptazyme to *in situ* sensor, a key concern is that some aptazymes show high blank self-cleavage activities even in the absence of target molecules, resulting in somewhat narrow linear range of detecting target molecules.

To reduce the blank self-cleavage activity, we fused aptamer moieties into the stem I and stem III regions of the hammerhead ribozyme to have a stable structure of the hammerhead ribozyme with lower degree of complementary base-pairing between the aptazyme main strand and the substrate strand. The bis-aptazyme did show a very low blank signal and hence high sensitivity, i.e. signal to noise ratio, to the target molecule. However, the mono-aptazyme having one aptamer unit either in the stem I, stem II or stem III region of the ribozyme did not show such properties. The special features of the bis-aptazyme appear to originate from allosteric conformational changes of the aptazyme upon binding to the target protein. There are two possibilities in its conformational changes. The one possibility is that although the complementary base-pairings between the bis-aptazyme and the substrate occur rapidly, the self-cleaving ribozyme activity is not shown yet in the absence of the target molecule owing to possibly long and flexible structure of the bis-aptazyme. But upon its binding with the target molecules, the bis-aptazyme changes into a rigid structure and induces its high ribozyme activity. The other possibility is that the conformational changes in the bis-aptazyme induced by its binding to the target molecule is quite fast, so that it increases the binding rate between the bis-aptazyme strand and the substrate, which subsequently enhances the ribozyme activity. The result of this report suggests that the latter possibility is more probable. It appears that the conformational change of the aptazymes triggered by the binding of the target molecule induces a faster binding of the main strand of the bis-aptazyme to the substrate strand.

To confirm the findings in our report, the stem II/III modified bis-aptazyme was also compared with the stem I/III modified bis-aptazyme. If the low blank signal from the stem I/III modified bis-aptazyme was caused only by the two aptamer-binding sites, i.e. binding of target molecule, the stem II/III modified bis-aptazyme should also exhibit the similar low blank signal. However, the stem II/III modified bis-aptazyme showed much higher blank signal, similar to that of the stem I, stem II or stem III modified mono-aptazymes (Supplementary Figure 4S). This result again supports that the positions of coupling the aptamer moiety and the number of the aptamers are important in the designing bis-aptazyme without blank signal.

Moreover, the newly designed bis-aptazyme in this study displayed slightly higher ribozyme activity than the corresponding other mono-aptazymes by 10–20%. One of the reasons of showing its higher catalytic activity would be that the bis-aptazyme having two binding sites for the target protein might have higher collision frequency compared with the mono-aptazyme under the same condition. The additional increase in the activity would be caused by faster releasing kinetics of the cleaved substrate owing to a reduction in the size of the complementary base-pairing sequences between the aptazyme main strand and the substrate.

This study on developing the bis-aptazyme with very low blank signal, but with high sensitivity and specificity for target protein would be meaningful in several points as follows: (i) *in situ* detection or analysis of target molecule is possible by designing a fusion aptazyme; (ii) secondary molecules such as secondary Ab and conjugated enzyme are not needed unlike

Ab-based analysis; (iii) general design principle can be always applied to any aptamers; (iv) more sensitive and versatile sensors can be designed; and (v) multiple sensors can be designed and so on. Further, versatile bis-aptazymes can be developed for protein and small molecule sensors in bio-MEMS, tools for proteomics (30), *in vivo*/*in vitro* medical diagnosis and prognosis, and tools for gene knock-out, gene regulation (31,32) and gene therapy (33).

SUPPLEMENTARY DATA

Supplementary Data are available at NAR Online.

ACKNOWLEDGEMENTS

We would like to thank Prof. Seong-Wook Lee in Dan-Kook University for kindly providing the vector for recombinant hepatitis C virus NS5b and NS3. This research was partially supported by the Intelligent Microsystems Project (IMP) in 21C Frontier R&D program, and Advanced Backbone IT Technology Development Project (IMT2000-B3-2) of the Ministry of Information and Communication. Funding to pay the Open Access publication charges for this article was provided by the Intelligent Microsystems Project (IMP) in 21C Frontier R&D program.

Conflict of interest statement. None declared.

REFERENCES

1. Urbain,J.L. (1999) Oncogenes, cancer and imaging. *J. Nucl. Med.*, **40**, 498–504.
2. Alaiya,A.A., Franzén,B., Auer,G. and Linder,S. (2000) Cancer proteomics: From identification of novel markers to creation of artifical learning models for tumor classification. *Electrophoresis*, **21**, 1210–1217.
3. Fang,X., Cao,Z., Beck,T. and Tan,W. (2001) Molecular aptamer for real-time oncoprotein platelet-derived growth factor monitoring by fluorescence anisotropy. *Anal. Chem.*, **73**, 5752–5757.
4. Famulok,M. and Mayer,G. (1999) Aptamers as tools in molecular biology and immunology. *Curr. Top. Microbiol. Immunol.*, **243**, 123–136.
5. Jhaveri,S., Rajendran,M. and Ellington,A.D. (2000) *In vitro* selection of signaling aptamers. *Nat. Biotechnol.*, **18**, 1293–1297.
6. Soukup,G.A. and Breaker,R.R. (1999) Engineering precision RNA molecular switches. *Proc. Natl Acad. Sci. USA*, **96**, 3584–3589.
7. Tang,J. and Breaker,R.R. (1997) Rational design of allosteric ribozymes. *Chem. Biol.*, **4**, 453–459.
8. Soukup,G.A. and Breaker,R.R. (1999) Design of allosteric hammerhead ribozymes activated by ligand-induced structure stabilization. *Struct. Fold. Des.*, **7**, 783–791.
9. Soukup,G.A., Emilsson,G.A. and Breaker,R.R. (2000) Altering molecular recognition of RNA aptamers by allosteric selection. *J. Mol. Biol.*, **298**, 623–632.
10. Tuerk,C. and Gold,L. (1990) Systematic evolution of ligands by exponential enrichment: RNA ligands to bacteriophage T4 DNA polymerase. *Science*, **249**, 505–510.
11. Peracchi,A., Beigelman,L., Usman,N. and Herschlag,D. (1996) Rescue of abasic hammerhead ribozymes by exogenous addition of specific bases. *Proc. Natl Acad. Sci. USA*, **93**, 11522–11527.
12. Wang,D.Y., Lai,B.H. and Sen,D. (2002) A general strategy for effector-mediated control of RNA-cleaving ribozymes and DNA enzymes. *J. Mol. Biol.*, **318**, 33–43.
13. Soukup,G.A. and Breaker,R.R. (1999) Engineering precision RNA molecular switches. *Proc. Natl Acad. Sci. USA*, **96**, 3584–3589.
14. Koizumi,M., Soukup,G.A., Kerr,J.N. and Breaker,R.R. (1999) Allosteric selection of ribozymes that respond to the second messengers cGMP and cAMP. *Nature Struct. Biol.*, **6**, 1062–1071.
15. Robertson,M.P. and Ellington,A.D. (2000) Design and optimization of effector-activated ribozyme ligases. *Nucleic Acids Res.*, **28**, 1751–1759.
16. Robertson,M.P. and Ellington,A.D. (2001) *In vitro* selection of nucleoprotein enzymes. *Nat. Biotechnol.*, **19**, 650–655.
17. Hartig,J.S., Najafi-Shoushtari,S.H., Grüne,I., Yan,A., Ellington,A.D. and Famulok,M. (2002) Protein-dependent ribozymes report molecular interactions in real time. *Nat. Biotechnol.*, **20**, 717–722.
18. Tang,J. and Breaker,R.R. (1997) Examination of the catalytic fitness of the hammerhead ribozyme by *in vitro* selection. *RNA*, **3**, 914–925.
19. Tang,J. and Breaker,R.R. (1998) Mechanism for allosteric inhibition of an ATP-sensitive ribozyme. *Nucleic Acids Res.*, **26**, 4214–4221.
20. Araki,M., Okuno,Y., Hara,Y. and Sugiura,Y. (1998) Allosteric regulation of a ribozyme activity through ligand-induced conformational change. *Nucleic Acids Res.*, **26**, 3379–3384.
21. Kertsburg,A. and Soukup,G.A. (2002) A versatile communication module for controlling RNA folding and catalysis. *Nucleic Acids Res.*, **30**, 4599–4606.
22. Cox,J.C. and Ellington,A.D. (2001) Automated selection of anti-protein aptamers. *Bioorg. Med. Chem.*, **9**, 2525–2531.
23. Lee,J.F., Hesselberth,J.R., Meyers,L.A. and Ellington,A.D. (2004) Aptamer database. *Nucleic Acids Res.*, **32**, D95–D100.
24. Tuschl,T. and Eckstein,F. (1993) Hammerhead ribozymes: importance of stem–loop II for activity. *Proc. Natl Acad. Sci. USA*, **90**, 6991–6994.
25. McCall,M.J., Hendry,P., Mir,A.A., Conaty,J., Brown,G. and Lockett,T.J. (2000) Small, efficient hammerhead ribozymes. *Mol. Biotechnol.*, **14**, 15–17.
26. Mathews,H., Sabina,J., Zuker,M. and Turner,D.H. (1999) Expanded sequence dependence of thermodynamic parameters improves prediction of RNA secondary structure. *J. Mol. Biol.*, **288**, 911–940.
27. Hormes,R. and Sczakiel,G. (2002) The size of hammerhead ribozymes is related to cleavage kinetics: the role of substrate length. *Biochimie*, **84**, 897–903.
28. Hwang,B., Cho,J.S., Yeo,H.J., Kim,J.H., Chung,K.M., Han,K., Jang,S.K. and Lee,S.W. (2004) Isolation of specific and high-affinity RNA aptamers against NS3 helicase domain of hepatitis C virus. *RNA*, **10**, 1277–1290.
29. Hertel,K.J., Herschlag,D. and Uhlenbeck,O.C. (1994) A kinetic and thermodynamic framework for the hammerhead ribozyme reaction. *Biochemistry*, **33**, 3374–3385.
30. Rudert,F. (2000) Genomics and proteomics tools for the clinic. *Curr. Opin. Mol. Ther.*, **2**, 633–642.
31. Bayer,T.S. and Smolke,C.D. (2005) Programmable ligand-controlled riboregulators of eukaryotic gene expression. *Nat. Biotechnol.*, **23**, 337–343.
32. Brantl,S. (2004) Bacterial gene regulation: from transcription attenuation to riboswitches and ribozymes. *Trends Microbiol.*, **12**, 473–475.
33. Bergeron,L.J. and Perreault,J.P. (2005) Target-dependent on/off switch increases ribozyme fidelity. *Nucleic Acids Res.*, **33**, 1240–1248.